Enhanced phosphorylation of Na-Cl cotransporter in experimental metabolic syndrome – role of insulin

Radko KOMERS, **Shaunessy ROGERS**, **Terry T. OYAMA**, **Bei XU**, **Chao-Ling YANG**, **James McCORMICK**, and **David H. ELLISON**
Division of Nephrology and Hypertension, Department of Medicine, Oregon Health and Science University. Portland, OR

Abstract

We investigated the activity of thiazide-sensitive sodium-chloride cotransporter (NCC) in experimental metabolic syndrome (MS) and the role of insulin in NCC activation. Renal responses to NCC inhibitor hydrochlorothiazide (HCTZ), as a measure of NCC activity *in vivo* were studied in 12-week old Zucker obese rats (ZO), a model of MS, and in lean control animals (ZL), together with renal NCC expression, and molecular markers of NCC activity, such as localization and phosphorylation. Effects of insulin were further studied in mammalian cell lines with inducible and endogenous expression of this molecule. ZO rats displayed marked hyperinsulinemia, but no differences in plasma aldosterone as compared to ZL. In ZO, natriuretic and diuretic responses to NCC inhibition with HCTZ were enhanced compared with ZL, and associated with a decrease in blood pressure (BP). ZO rats displayed enhanced Thr53 NCC phosphorylation and predominant membrane localization of both total and phosphorylated NCC, together with a different profile in expression of SPAK isoforms, and lower expression of WNK4. *In vitro*, insulin induced NCC phosphorylation, which was blocked by PI3 kinase inhibitor. Insulin-induced reduction in WNK4 expression was also observed, but delayed compared with the time course of NCC phosphorylation. In summary, we report increased NCC activity in hyperinsulinemic rodents in conjunction with SPAK expression profile consistent with NCC activation and reduced WNK4 as well as an ability of insulin to induce NCC stimulatory phosphorylation *in vitro.* Together, these findings indicate that hyperinsulinemia is an important driving force of NCC activity in MS with possible consequences for BP regulation.

Keywords

thiazide-sensitive sodium-chloride cotransporter; metabolic syndrome; insulin; Zucker obese rat; WNK4

Address for correspondence: Radko Komers, MD, PhD, Division of Nephrology and Hypertension, Oregon Health & Science University, 3303 SW Bond Ave., CH12R, 97239 Portland, OR, Tel.: 503 721 7997, Fax: 503 721 7810, komersr@ohsu.edu.

INTRODUCTION

In insulin resistant (IR) states, elevated plasma insulin levels develop due to resistance to insulin-stimulated glucose uptake in traditional sites of its actions, such as the skeletal muscle, liver or adipose tissue, and can act on various other tissues with harmful consequences [1]. The kidney is one of possible targets of these actions. Insulin receptors are expressed along the nephron, and insulin increases the reabsorptive activity of major renal sodium transporter proteins [2]. Indeed, the ability of insulin to stimulate sodium retention in the kidney [2,3] has been shown to be unaffected [4–7], or even increased in IR states [7].

In affected individuals, IR develops as part metabolic syndrome (MS), together with Type 2 diabetes (DM2), truncal obesity, lipid abnormalities, and with the development of hypertension [8]. Numerous experimental and clinical studies have investigated pathways that connect MS with hypertension. However, the links between the mentioned metabolic factors and elevations of blood pressure (BP) remain elusive.

Zucker obese rats (ZO), a model of MS, IR and hyperinsulinemia, display early (2–4 months of age) increases in the abundance of several sodium transporters [9,10]. Our previous work [11], in accord with work by others [12], has shown enhanced activity of the components of the insulin signaling cascade, such as Akt kinase, in the kidney in hyperinsulinemic models of IR. Insulin also activates serum/glucocorticoid regulated kinase 1 (SGK-1) in the distal nephron leading to antinatriuresis mediated by ENaC via the insulin-like growth factor-I (IGF-I) receptor [13,14]. These phenomena provide possible mechanisms for the development of hypertension in the MS.

The thiazide-sensitive sodium-chloride cotransporter (NCC), the main sodium transporter in the distal convoluted tubule (DCT), is responsible for reabsorption of 3–7% of filtered sodium load. NCC expression is limited to DCT cells both at the mRNA and protein level [15]. The NCC activity is modulated by aldosterone, angiotensin II, tonicity and tubular flow [16–22]. In addition, there is emerging evidence that NCC could be a target of insulin actions. Several studies conducted in different experimental conditions have suggested that insulin-induced increases in activity and/or abundance of NCC in the DCT may play a role in blood pressure (BP) elevations in rodents [10,21,23,24]. Altogether, these data suggest that NCC activation in IR states may contribute to sodium retention.

Phosphorylation of NCC along its amino terminal cytoplasmic domain is essential for full cotransporter activity [17,25,26]. Studies conducted during the past decade have shown that the NCC is modulated by a signaling complex involving the WNK (*with no lysine*) kinases. WNK kinases modulate activity of STE 20-related proline-alanine-rich kinase (SPAK)/ oxidative stress-response kinase 1 (OSR1) [27–30], which in turn can directly phosphorylate NCC [17,26]. WNK4 has attracted recent attention as a possible modulator of hormonal actions on NCC [18,30,31]. WNK4 appears to be able to exert either inhibitory or stimulatory actions on NCC, depending on the underlying physiological state and the level of angiotensin II [32]. Additional lines of evidence have indicated that important intermediates in the insulin signaling cascade, such as Akt or SGK1, operate upstream of, or interact with, the WNK-SPAK/OSR1 signaling complex [18,33]. Therefore, it is likely that insulin induces NCC activity via phosphorylation on SPAK/OSR1-dependent residues.

Here, we tested the hypothesis that hyperinsulinemia in IR states stimulates NCC activity by enhancing its phosphorylation at SPAK/OSR1-dependent sites. To address this issue, we determined NCC activity in hyperinsulinemic ZO rats as compared to normoinsulinemic lean control animals. Renal responses to the NCC inhibitor hydrochlorothiazide (HCTZ)

were investigated as a measure of NCC activity *in vivo* in conjunction with renal abundance and membrane translocation of total and phosphorylated NCC, and expression of its modulators, SPAK and WNK4. To directly determine whether insulin itself could participate in NCC phosphorylation, we reproduced the results *in vitro* in mammalian cell lines.

METHODS

Animals

Studies were performed in 16 ZO and 16 Zucker lean (ZL) rats, which do not display any metabolic defects. The animals were obtained from Charles River (Wilmington, MA). Zucker obese rats have a defect in leptin receptor that leads to hyperphagia and the development of obesity and IR within several weeks of age [34,35]. The animals were housed with a light-dark cycle of 12 hours each, and with free access to food (standard chow) and water. All experiments were carried out with the approval of, and in accordance with the regulations of the local IACUC Committee.

In vivo studies

The experiment was initiated in 10 weeks old rats. The animals were administered with a vehicle (0.9% NaCl, 200 μl i.p.) and placed into metabolic cages for 24-hour collection of urine allowing measurements of urinary excretion of sodium ($U_{Na}V$) and potassium (U_KV), as well as urinary flow (UF). This 24-hour period was divided into 2 collection periods, allowing the measurements of early 0–3 hour (9.00 a.m.– noon) and 4–24 hour excretory responses. After completion of measurements in metabolic cages, the rats received second dose of the vehicle and within the 2 hours underwent measurements of systolic blood pressure by tail plethysmography as previously described [36]. The same day of the following week, the measurements were repeated in a similar manner to assess the responses to hydrochlorothiazide HCTZ (3.75 mg/kg i.p. in 200 μl 0.9% NaCl) before 24-hour urine collection followed by the second dose within 2 hours before BP measurements) as a measure NCC activity *in vivo*. To account for hyperphagia characteristic for the ZO rats, food intake was monitored during the urine collection periods as a possible confounding factor in renal excretory function studies. The experiment was completed by kidney harvesting for molecular studies at week 12.

Tissue harvesting for immunoblotting and immunofluorescence

The rats were anesthetized with thiobarbiturate (Inactin, Sigma, St. Louis, MO, 100 mg/kg, i.p.) and the abdominal aorta was exposed via midabdominal incision. The aorta was cannulated with the PE-50 catheter 3–5 mm above the bifurcation, and the catheter was fed to the orifice of left renal artery. The right renal artery was ligated and the right kidney was removed, decapsulated, divided into cortical and medullary portions, and snap frozen in liquid nitrogen for western blot analysis. Left kidney was then perfused retrogradely with PBS/sucrose adjusted to 330 mosmol/kgH2O, pH 7.4, for 20 s, followed by perfusion-fixation with 3% paraformaldehyde in PBS for 5 min. After perfusion, the kidney was removed, cut transversely into 3mm sections and cryopreserved overnight in 800mOsm sucrose/PBS solution at 4 degrees. The kidney sections were then snap-frozen in isopentane cooled with dry ice.

Cell culture and in vitro experiments

Tetracycline-inducible Human Embryonic Kidney 293 (HEK293) NCC Cells—
cDNA encoding full-length mouse NCC was subcloned into the pcDNA5/FRT/TO vector (Invitrogen). FlpIn 293 host cells (Invitrogen) were cotransfected with the pcDNA5/FRT/TO-NCC construct and pOG44, a plasmid expressing Flp recombinase, resulting in a

homologous recombination event. Transfected cells were screened for hygromycin resistance and lack of β–galactosidase activity. The Flp-In T-REx 293 NCC (Flp-In NCC) cell line was maintained in high-glucose DMEM containing 10% FBS, 200 µg/ml hygromycin, 15 µg/ml blasticidin, and penicillin/streptomycin. NCC induction was confirmed by incubating the cells with or without tetracycline (TTC, 1 µg/ml), followed by cell lysis and western blotting. Endogenous expression of SPAK/OSR1 in HEK293 cells was described previously [37].

The cells were grown in insulin-free DMEM with 5.5 mM glucose, supplemented with 10% fetal bovine serum and antibiotics. Uninduced cells were harvested for western blots as negative controls. To study the effect of insulin on NCC phosphorylation, the cells were first stimulated with TTC to induce NCC expression. Eighteen hours after NCC induction the cells were treated with insulin (40 ng/ml) and harvested after 10–360 minutes for further analyses by immunoblotting with anti-NCC and anti-phospho-NCC antibodies.

To further explore the insulin-induced signaling pathways leading to NCC phosphorylation, the effects of insulin were investigated as above in TTC-induced cells with or without pretreatment with the phosphatidyl-inositol-3 kinase (PI3K) inhibitor LY294002 (60 min., 50 µM; Cayman Chemical Company, Ann Arbor, MI).

Mouse distal convoluted tubule (MDCT) cells—The MDCT cells (a gift from Dr. Peter A. Friedman, University of Pittsburgh) were used as another *in vitro* mammalian cell model, which displays endogenous NCC and WNK4 expression [38,39]. The cells were stimulated with insulin for 20, 40 and 240 minutes with or without pretreatment with PI3K inhibitor LY294002 (60 min., 50 µM). Additional analyses were conducted in cells 24–48 hours after insulin stimulation and compared to cells grown in insulin-free media. The culture conditions and processing for further analyses was same as in Flp In-NCC cells. All *in vitro* studies were performed at least in quadruplicate.

Immunoblotting and immunofluorescence

The kidney cortical samples or cells were homogenized and processed to obtain whole-cell or crude membrane samples (100000g pellet) and analyzed by immunoblotting as previously described [40], using primary rabbit custom antisera directed against NCC (1:5000), anti–phospho NCC, WNK4 (Phosphosolutions, Aurora, CO) [41], C-terminal SPAK (C-SPAK) [42], N-terminal SPAK (N-SPAK) [43] or rabbit primary antibodies raised against anti-phospho Ser 473 Akt (P-Akt, Cell Signaling, 1:500), followed HRP-conjugated secondary antibodies (Pierce). The phospho-NCC antibody recognizes phosphorylated Thr53 of rat NCC one of several functionally important sites of amino terminal phosphorylation [17,26]. Visualization, loading control and image analysis were accomplished as described previously [40].

Same rabbit antisera directed against NCC and P-NCC were used. Sets of 5 micron cryostat sections from pairs of ZL and ZO rats were processed exactly in the same fashion. The sections were washed 3 times in PBS before permeabilization in 0.5% Triton-X in PBS for 30 minutes. The sections were again washed before being incubated with blocking medium 5% milk in PBS (30 min), followed by primary antibodies diluted in blocking medium (1 h). Fluorescent secondary antibodies (Zymed-Invitrogen, Carlsbad, Ca) were applied for detection. Sections were mounted in VectaShield HardSet Mounting Medium (Vector Labs, Burlingame CA) and evaluated in a Leica DMRB microscope.

Biochemical methods

Urinary sodium and potassium were measured by EL-ISE autoanalyser (Beckman, Brea, CA). Plasma insulin and aldosterone concentrations were analyzed by ELISA (ALPCO, Salem, NH resp. Immuno-biological Laboratories USA, Minneapolis, MN). Blood glucose was measured using a reflectance meter (One Touch II; Lifescan, Milpetas, California, USA).

Statistical analysis

Data are expressed as means ± SEM. Inter-group analyses were performed by ANOVA factorial with Bonferroni's post test. Two-way ANOVA was also applied to further analyze the effect of body type on phospho-NCC abundance in the renal cortex. Statistical significance was defined as a p value < 0.05.

RESULTS

Zucker obese rats display enhanced renal excretory response to HCTZ

General physical characteristics and metabolic/hormonal parameters are shown in Table 1. At 12 weeks of age, ZO rats displayed increased body and kidney weight, and mild but significant increases in BG levels as compared to ZL rats. Plasma insulin levels were markedly elevated in ZO, whereas plasma aldosterone concentrations were similar in ZL and ZO animals.

The rates of urinary sodium excretion, during the vehicle administration and after HCTZ are shown in Figure 1. There were no differences in $U_{Na}V$ between the ZL and ZO rats following the administration of a vehicle. HCTZ increased early $U_{Na}V$ (0–3 hours) in both ZL and ZO rats, but the response was markedly enhanced in obese animals. Since the response to a diuretic is typically followed by a period of enhanced sodium reabsorption, we also analyzed $U_{Na}V$ during the rest of the 24-hour collection periods (hours 4–24). During this period, there were no differences in $U_{Na}V$ between the ZL and ZO rats after vehicle administration, but the difference in natriuretic response to HCTZ (right panels) between the groups was still apparent. The differences in early natriuresis (0–3 hours) between the ZO and ZL animals were also present when the data were expressed as ratios per body weight.

Both early and 4–24 hour UF and U_KV following the vehicle administration were higher in ZO than in ZL rats (Figure 1). The effects of HCTZ on UF and U_KV during the 0–3 hour collection period followed the same pattern as $U_{Na}V$ with greater responses observed in ZO as compared to lean counterparts. In addition, ZO rats demonstrated higher UF and U_KV after HCTZ during the 4–24 hour period. When adjusted for body weight, significantly higher diuretic and kaliuretic responses in ZO was observed only during the initial collection period.

The food intake during the control experiment (vehicle) was not different between the ZL and ZO animals (ZL: 19±2 vs. ZO: 22±2 g; p=n.s.), but was significantly higher during the urine collection after the administration of HCTZ (ZL: 17±2 vs. ZO: 32±3 g; p<0.05). During the early collection period (0–3 h.), all rats had negligible food intake and this factor did not influence observed differences in excretory responses to HCTZ. When adjusted for food intake, there were no differences in 4–24 hour $U_{Na}V$ between the ZL and ZO rats both after the vehicle or HCTZ administration (vehicle: ZL, 54±3 vs. ZO, 70±14 µmol/24hours/g of food; HCTZ: ZL, 54±4 vs. ZO, 42±4 µmol/24hours/g of food p=n.s.), as well as in 24-hour UF and U_KV (not shown).

Although blood pressures were similar in ZL and ZO animals at baseline, HCTZ treatment reduced BP only in ZO rats (p<0.05, Figure 2).

Renal cortical NCC and WNK4

Although renal cortical NCC abundance was not different between the ZL and ZO rats (Figure 3, Panels A, C), the abundance of NCC in crude membrane fractions was higher in obese than in lean animals (Figure 3, Panels A, C). The NCC phosphorylation at several threonine residues has been shown to be one of mechanisms required for its activation [17]. The abundance of P-NCC (phosphorylated at Th53) was increased markedly in membrane fractions from ZO compared with ZL animals (Figure 3, Panels B and C); a similar trend was observed in renal cortical whole cell homogenates (p=0.07, Fig. 3, Panels B and C). When expressed as a ratio of phospho- to total NCC in corresponding samples, the differences between the ZL and ZO rats were apparent in both fractions (Figure 3, Panel C).

NCC activity can be regulated by insertion and removal from the apical membrane. Unlike the ZL, which displayed diffuse and more prominent cytoplasmic distribution of NCC, ZO rats demonstrated predominant apical membrane NCC distribution (Fig. 3D). This pattern in lean and obese animals was even more apparent for phosphorylated NCC.

As noted, WNK4 and SPAK are known to regulate NCC activity [17,26,43]. Therefore, following analyses determined protein expression of these molecules. Immunoblotting using the antibody directed against the C-terminus of SPAK (C-SPAK) revealed several bands (Fig. 3E). Densitometric analysis of all bands did not show any differences between ZL and ZO animals. In contrast, the band with the highest molecular weight (~ 60 kD), corresponding to full size SPAK (FL-SPAK), was significantly more abundant in ZO rats (Fig. 3E). The following analysis of kidney homogenates using an antibody directed against N-terminal of SPAK, which detects only FL-SPAK [43], revealed a weak signal at a molecular weight corresponding to this protein only in renal cortices from ZO, but not ZL rats (Fig. 3E). As shown in Fig. 3F, renal cortical WNK4 abundance was reduced ZO rats compared with lean controls.

Effects of insulin on NCC and WNK4 *in vitro*

Having established the association of hyperinsulinemia with increased NCC activity and phosphorylation in vivo in IR rats, we conducted further studies to provide direct evidence for insulin-induced phosphorylation NCC *in vitro*.

The effects of insulin on NCC Thr53/55 phosphorylation (P-NCC) were first investigated in Flp-In NCC cells with inducible overexpression of NCC. As expected, NCC was not found in uninduced cells (UI, Figure 4A). The cells induced by TTC were harvested at baseline and at subsequent time points indicated in Figure 4A. P-NCC was barely detectable at baseline. Insulin stimulation lead to a sustained phosphorylation of NCC detectable at 20 min. after the stimulation (Fig. 4A,B). The abundance of total NCC remained stable during the observation period resulting in an increase in the ratio of phospho- and total NCC apparent at 40 min. after stimulation (Figure 4B). The Ser473 phosphorylation of Akt kinase, a key molecule in insulin signaling cascade [44], was barely detectable in uninduced and in induced Flp-In NCC cells at baseline. Strong Akt phosphorylation was apparent already at 10 min. after insulin stimulation and preceded the phosphorylation of NCC (Fig. 4C). Insulin-induced NCC phosphorylation was markedly attenuated by pretreatment with LY294002 (Fig. 4D,E), the inhibitor of PI3K, a kinase operating upstream of Akt in insulin signaling cascade [44]. Insulin-induced Ser473 phosphorylation of Akt was not detectable in LY294002-treated Flp-In NCC cells (Fig. 4F).

Further experiments were performed in primary MDCT with endogenous expression of NCC and WNK4. The effect of insulin on NCC phosphorylation in MDCT reproduced the observations in Flp-In HEK293 cells (Fig. 5A,B). Stimulation with insulin lead to a gradual decrease in WNK4 protein expression with a significant difference after 240 min. as compared to baseline (Fig. 5C). The insulin-induced decrease in WNK4 was not detected in MDCT cells, which were pretreated by LY294002 (Fig. 5D). Lower WNK4 was detectable also after 24 and 48 hours in insulin-treated cells when compared to time controls grown in insulin-free-media (Fig. 5E).

DISCUSSION

The current results show that ZO rats exhibit enhanced natriuretic, diuretic and kaliuretic responses to NCC inhibition with HCTZ, as compared to their lean counterparts. These responses were associated with an increase in the abundance of NCC protein in crude membrane fractions in renal cortical samples from ZO rats, studied as one of surrogate markers of NCC activity [22,45–47]. The ZO rats were studied at 10–12 weeks of age i.e., at a prehypertensive stage, to avoid confounding effects of BP on baseline natriuresis. According to most studies, this model develops significantly elevated BP at 18–20 weeks of age [24]. Despite this fact, we observed BP-lowering effect of HCTZ in ZO, but not ZL, rats. At this early time point, a component of direct vasodilation may have contributed to the BP-lowering effect of HCTZ [48]. Yet, we consider early natriuresis the major driving force of the BP-lowering effect of HCTZ, as it was observed only in the ZO animals, which demonstrated strikingly enhanced natriuretic effects. We are not aware of data indicating enhanced vasodilator responses to HCTZ in resistance arteries in IR states.

While these observations correspond to previous work by others [10,22,24,45–47,49,50] here we also provide new evidence that NCC is further activated via phosphorylation in IR ZO animals. As noted, phosphorylation of NCC at several sites along its amino terminal cytoplasmic regulatory domain enhances transporter activity, independent of protein abundance; conversely, mutation of three phosphorylation sites (Thr53, Thr58, and Ser71 sites [17,25,26]) renders the protein virtually inactive. Although the relationship between phosphorylation and translocation to the plasma membrane remains unclear, it appears that the fully activated, membrane associated protein is the phosphorylated species [17] and that the abundance of phosphorylated NCC can be considered to be a marker of NCC activity [47].

Compared to ZL rats, NCC phosphorylation in ZO rats was increased, in particular in membrane fractions. Moreover, localization of P-NCC in the DCT using the IF showed predominant apical membrane distribution in ZO rat kidneys, consistent with the active pool of the cotransporter. Altogether, these observations indicate enhanced NCC activity at this stage of MS.

Despite the emerging evidence of altered regulation of the NCC in experimental MS, the nature of the upstream signals responsible for this phenomenon remains unknown. The pattern of NCC expression observed in the present study corresponds to other findings in *in vivo* studies exploring the effects hormonal stimulators such as aldosterone [51], Ang II [20,30,51] or vasopressin [47].

Previous studies have attempted to link increases in NCC activity in ZO rats to AngII actions [49]. The natriuretic responses to HCTZ were attenuated by AngII receptor blockade with candesartan suggesting the contribution of the peptide to NCC activation. However, the sensitivity to candesartan was similar in ZO and ZL indicating that, although the NCC is under the control of AngII, this mechanism it is not specific for ZO rats and does not explain

different responses to HCTZ between lean and obese rats. Aldosterone is another mediator that could participate in NCC activation in ZO rats, but the lack of differences in plasma aldosterone between the lean and obese animals does not support its role, at least in this model.

In 12-week old ZO, hyperinsulinemia appears to be the most prominent hormonal abnormality with respect to sodium handling. Several lines of evidence in hyperinsulinemic IR rats suggest that NCC may be a direct target of insulin action. In normal rats, insulin infusion enhances natriuretic response to HCTZ [23]. Treatment with an insulin-sensitizing compound rosiglitazone, which reduces plasma insulin levels in ZO rats, reduces the natriuretic response to HCTZ, suggesting that the suppression of insulin levels reduces NCC activity [10]. Additionally, SGK1, which can be activated by insulin, may contribute to the enhanced expression and activation of the NCC [21,50].

A key signaling pathway that modulates NaCl reabsorption involves WNK kinases interacting with SPAK and OSR1 [17,26–28]. In mammalian cells, SPAK phosphorylates and activates cation chloride cotransporters, including NCC [17,26]. McCormick et al. [43] recently identified a kidney-specific SPAK isoform (KS-SPAK), which lacks the kinase domain and inhibits NCC and NKCC phosphorylation by FL-SPAK in vitro. The KS-SPAK has been localized predominantly in TALH, whereas the FL-SPAK is more abundantly expressed along the DCT. These workers also reported a SPAK "isoform switch" in response to Na restriction (a state of NCC and NKCC2 activation) characterized by enhanced expression of FL-SPAK and suppressed KS-SPAK; these changes would be expected to facilitate NaCl reabsorption along both THAL and DCT.

In accord with observations in the mouse kidney [43], the present analysis revealed several SPAK bands also in rat kidneys. The FL-SPAK, which has been considered as the only form capable of phosphorylating NCC, was more abundant in ZO animals. The N-terminal SPAK antibody has been used to identify the NCC-stimulating component of SPAK (FL-SPAK), as other SPAK isoforms lack the recognized epitope. Although the signal detected from kidney tissue homogenates using this antibody is relatively weak, we detected a stronger 60–65 kD band, corresponding to FL-SPAK, in ZO rat kidneys, suggesting that the more abundant kinase-active, full length, SPAK contributes to the greater abundance of activated NCC. The band with the lowest molecular weight, detected using the C-terminal antibody in the present analysis, might correspond to KS-SPAK in mice. Although not a focus of the present study, the mentioned isoform shift was apparent in also in ZO rats (Fig. 3F, C-SPAK).

The role of WNK4 is still controversial, as both inhibitory and stimulatory effects on NCC have been proposed. Accordingly, some physiological perturbations that lead to decreases in NCC have been associated with increases in WNK4, whereas other stimuli, such as angiotensin II infusion, appear to convert WNK4 from an inhibitory to a stimulatory state. In the present study, the more abundant P-NCC in ZO rats was associated with a lower abundance of WNK4; whether this difference is causal or consequential requires further study.

Because the observations in rats are largely indirect and inferential, as whole animal responses to perturbation elicit multiple effects, we therefore tested effects of insulin on NCC *in vitro,* using 2 different mammalian cell models. The cells were stimulated with insulin at a concentration corresponding to average plasma insulin levels observed in ZO rats. The increase in phosphorylated NCC, together with activation of Akt kinase, a key molecule in insulin signaling cascade, was clearly apparent in the Flp-In NCC cells 20 minutes after insulin stimulation; this increase was sustained for at least 4 hours. The effects of insulin on NCC were attenuated, and in case of Akt abolished, by pretreatment of cells

with the PI3K inhibitor LY294002. This observation shows that PI3K-Akt operates upstream of NCC in insulin-induced activation pathway. Notably, previous studies by others [12] and by our group [11] in IR hyperinsulinemic rodent models have demonstrated increased renal Akt activity as compared to control animals, and its normalization by PI3K inhibition [11].

The effects of insulin were further studied in MDCT cells with endogenous NCC and WNK4 expression. The results were similar to those observed in the Flip-In NCC cells, as insulin-treatment increased the abundance of P-NCC. Having observed a decrease in WNK4 in ZO rats, we sought to determine whether this phenomenon could be reproduced in insulin-stimulated cells. Indeed, the insulin stimulation that led to an increase in P-NCC abundance in MDCT cells also caused a decrease in WNK4 abundance; this was not observed in insulin-stimulated cells pretreated with PI3K inhibitor. The decrease in WNK4 in response to insulin was rather delayed, however, as compared to insulin-induced NCC phosphorylation. Consequently, it does not seem likely that a reduction in WNK4 causes the early NCC activation by the hormone, but suggests instead that WNK4 either helps maintain NCC in an activated state during chronic hyperinsulinemia (in its inhibitory mode) or acts as a counter regulatory factor (in its stimulatory mode; see below). At this stage, we can only speculate about the mechanisms of insulin-induced WNK4 downregulation, which seems to be too rapid to involve transcriptional events, but can involve protein degradation as described for other components of this pathway [52].

Combining the *in vitro* experiments in mpkDCT cells with *in vivo* approaches in mice, Sohara et al. [53] have recently reported stimulatory effect of insulin on SPAK and NCC phosphorylation via PI3K. The effects of insulin were abolished in cells with SPAK or WNK4 knockdown, as well as in mice with SPAK deletion and in WNK4 hypomorphic mice. In most aspects, our observations are in accord with this report. It has been suggested that hormones, such as Ang II [20,30] or aldosterone [18], activate NCC at least in part by converting WNK4 to an NCC-stimulatory mode. In this respect, our observation that P-NCC increases before any change in WNK4 abundance, and the report of Sohara and colleagues suggesting that WNK4 is necessary for the insulin-induced stimulation, together suggest that insulin may shift WNK4 to its stimulatory mode, in a manner analogous to AngII; in this case, the late decline in WNK4 abundance may be compensatory.

There are, however, important differences between these two studies that make direct comparison difficult: *In vitro*, Sohara et al. [53] stimulated the cells with 100 nM of insulin, i.e. a concentration ~100 times above the physiological range. In contrast, our experiments were conducted in cells stimulated with insulin concentration found in hyperinsulinemic animals (~7–8 nM), which are already markedly elevated as compared to normal rats or humans. The impact of supraphysiological insulin levels on phosphorylation cascades leading to NCC activation may not reflect *in vivo* conditions. Our observations in rats reflect chronic hyperinsulinemia, whereas the former study addressed acute effects of the hormone. Finally, the WNK4 hypomorphic mice are not true knockout animals and express portions of the WNK4 molecule that may be functional [54,55].

In summary, we report enhanced natriuretic, diuretic and BP responses to inhibition of the NCC in IR hyperinsulinemic ZO rats as compared to lean counterparts. These responses were in ZO rats associated with molecular indicators of NCC activation, an increase in FL-SPAK expression and reduced expression of WNK4, a negative regulator of NCC. The stimulation of NCC-expressing cells *in vitro* with insulin at a concentration matching the plasma levels observed in ZO rats resulted in NCC phosphorylation mediated at least in part by Akt kinase and followed by a reduction of WNK4 expression, a pattern also observed in vivo. The data indicate that hyperinsulinemia is the major driving force of observed

differences in NCC activity and expression between the ZL and ZO rats with possible consequences for BP regulation. A downregulation of WNK4 may help to maintain NCC in an activated state during chronic hyperinsulinemia.

Acknowledgments

List of abbreviations

|	
DCT	distal convoluted tubule
DM2	Type 2 diabetes
HCTZ	hydrochlorothiazide
IGF-I	insulin-like growth factor-I
IR	insulin resistance
MDCT	mouse distal convoluted tubule cells
MS	metabolic syndrome
NCC	sodium-chloride cotransporter
OSR1	oxidative stress-response kinase 1
PI3K	phosphatidyl inositol 3 kinase
SGK-1	serum/glucocorticoid regulated kinase 1
SPAK	STE 20-related proline-alanine-rich kinase (SPAK)
$U_{Na}V$	urinary excretion of sodium
U_KV	urinary excretion of potassium
UF	urinary flow
WNK	(*with no lysine*) kinase
ZL	Zucker lean rat
ZO	Zucker obese rat.

References

1. Sarafidis PA, Bakris GL. The antinatriuretic effect of insulin: an unappreciated mechanism for hypertension associated with insulin resistance? Am J Nephrol. 2007; 27:44–54. [PubMed: 17245074]

2. Tiwari S, Riazi S, Ecelbarger CA. Insulin's impact on renal sodium transport and blood pressure in health, obesity, and diabetes. Am J Physiol Renal Physiol. 2007; 293:F974–984. [PubMed: 17686957]

3. Gupta AK, Clark RV, Kirchner KA. Effects of insulin on renal sodium excretion. Hypertension. 1992; 19(Suppl 1):178–182.

4. Rocchini AP, Katch V, Kveselis D, Moorehead C, Martin M, Lampman R, Gregory M. Insulin and renal sodium retention in obese adolescents. Hypertension. 1989; 14:367–374. [PubMed: 2676858]

5. Natali A, Quinones Galvan A, Santoro D, Pecori N, Taddei S, Salvetti A, Ferrannini E. Relationship between insulin release, antinatriuresis and hypokalaemia after glucose ingestion in normal and hypertensive man. Clin Sci. 1993; 85:327–335. [PubMed: 8403806]

6. Nosadini R, Sambataro M, Thomaseth K, Pacini G, Cipollina MR, Brocco E, Solini A, Carraro A, Velussi M, Frigato F, et al. Role of hyperglycemia and insulin resistance in determining sodium retention in non-insulin-dependent diabetes. Kidney Int. 1993; 44:139–146. [PubMed: 8355455]

7. Sechi LA. Mechanisms of insulin resistance in rat models of hypertension and their relationships with salt sensitivity. J Hypertens. 1999; 17:1229–1237. [PubMed: 10489099]

8. Sowers JR, Standley PR, Ram JL, Zemel MB, Resnick LM. Insulin resistance, carbohydrate metabolism, and hypertension. Am J Hypertens. 1991; 4:466S–472S. [PubMed: 1832873]

9. Bickel CA, Knepper MA, Verbalis JG, Ecelbarger CA. Dysregulation of renal salt and water transport proteins in diabetic Zucker rats. Kidney Int. 2002; 61:2099–2110. [PubMed: 12028450]

10. Khan O, Riazi S, Hu X, Song J, Wade JB, Ecelbarger CA. Regulation of the renal thiazide-sensitive Na-Cl cotransporter, blood pressure, and natriuresis in obese Zucker rats treated with rosiglitazone. Am J Physiol Renal Physiol. 2005; 289:F442–450. [PubMed: 15814531]

11. Zdychova J, Kazdova L, Pelikanova T, Lindsley JN, Anderson S, Komers R. Renal activity of Akt kinase in obese Zucker rats. Exp Biol Med (Maywood). 2008; 233:1231–1241. [PubMed: 18641049]

12. Feliers D, Duraisamy S, Faulkner JL, Duch J, Lee AV, Abboud HE, Choudhury GG, Kasinath BS. Activation of renal signaling pathways in db/db mice with type 2 diabetes. Kidney Int. 2001; 60:495–504. [PubMed: 11473632]

13. Gonzalez-Rodriguez E, Gaeggeler HP, Rossier BC. IGF-1 vs insulin: respective roles in modulating sodium transport via the PI-3 kinase/Sgk1 pathway in a cortical collecting duct cell line. Kidney Int. 2007; 71:116–125. [PubMed: 17164836]

14. Huang DY, Boini KM, Friedrich B, Metzger M, Just L, Osswald H, Wulff P, Kuhl D, Vallon V, Lang F. Blunted hypertensive effect of combined fructose and high-salt diet in gene-targeted mice lacking functional serum- and glucocorticoid-inducible kinase SGK1. Am J Physiol Regul Integr Comp Physiol. 2006; 290:R935–944. [PubMed: 16284089]

15. Bachmann S, Velazquez H, Obermuller N, Reilly RF, Moser D, Ellison DH. Expression of the thiazide-sensitive Na-Cl cotransporter by rabbit distal convoluted tubule cells. J Clin Invest. 1995; 96:2510–2514. [PubMed: 7593642]

16. Kim GH, Masilamani S, Turner R, Mitchell C, Wade JB, Knepper MA. The thiazide-sensitive Na-Cl cotransporter is an aldosterone-induced protein. Proc Natl Acad Sci U S A. 1998; 95:14552–14557. [PubMed: 9826738]

17. Richardson C, Alessi DR. The regulation of salt transport and blood pressure by the WNK-SPAK/OSR1 signalling pathway. J Cell Sci. 2008; 121:3293–3304. [PubMed: 18843116]

18. Rozansky DJ, Cornwall T, Subramanya AR, Rogers S, Yang YF, David LL, Zhu X, Yang CL, Ellison DH. Aldosterone mediates activation of the thiazide-sensitive Na-Cl cotransporter through an SGK1 and WNK4 signaling pathway. J Clin Invest. 2009; 119:2601–2612. [PubMed: 19690383]

19. Chiga M, Rai T, Yang SS, Ohta A, Takizawa T, Sasaki S, Uchida S. Dietary salt regulates the phosphorylation of OSR1/SPAK kinases and the sodium chloride cotransporter through aldosterone. Kidney Int. 2008; 74:1403–1409. [PubMed: 18800028]

20. Talati G, Ohta A, Rai T, Sohara E, Naito S, Vandewalle A, Sasaki S, Uchida S. Effect of angiotensin II on the WNK-OSR1/SPAK-NCC phosphorylation cascade in cultured mpkDCT cells and in vivo mouse kidney. Biochem Biophys Res Commun. 2010; 393:844–848. [PubMed: 20175999]

21. Vallon V, Schroth J, Lang F, Kuhl D, Uchida S. Expression and phosphorylation of the Na+-Cl-cotransporter NCC in vivo is regulated by dietary salt, potassium, and SGK1. Am J Physiol Renal Physiol. 2009; 297:F704–712. [PubMed: 19570885]

22. Sandberg MB, Riquier AD, Pihakaski-Maunsbach K, McDonough AA, Maunsbach AB. ANG II provokes acute trafficking of distal tubule Na+-Cl(−) cotransporter to apical membrane. Am J Physiol Renal Physiol. 2007; 293:F662–669. [PubMed: 17507603]

23. Song J, Hu X, Riazi S, Tiwari S, Wade JB, Ecelbarger CA. Regulation of blood pressure, the epithelial sodium channel (ENaC), and other key renal sodium transporters by chronic insulin infusion in rats. Am J Physiol Renal Physiol. 2006; 290:F1055–1064. [PubMed: 16303859]

24. Osmond JM, Mintz JD, Stepp DW. Preventing increased blood pressure in the obese Zucker rat improves severity of stroke. Am J Physiol Heart Circ Physiol. 2010; 299:H55–61. [PubMed: 20418477]

25. Pacheco-Alvarez D, Cristobal PS, Meade P, Moreno E, Vazquez N, Munoz E, Diaz A, Juarez ME, Gimenez I, Gamba G. The Na+:Cl- cotransporter is activated and phosphorylated at the amino-terminal domain upon intracellular chloride depletion. J Biol Chem. 2006; 281:28755–28763. [PubMed: 16887815]

26. Richardson C, Rafiqi FH, Karlsson HK, Moleleki N, Vandewalle A, Campbell DG, Morrice NA, Alessi DR. Activation of the thiazide-sensitive Na+-Cl- cotransporter by the WNK-regulated kinases SPAK and OSR1. J Cell Sci. 2008; 121:675–684. [PubMed: 18270262]

27. Kahle KT, Rinehart J, Giebisch G, Gamba G, Hebert SC, Lifton RP. A novel protein kinase signaling pathway essential for blood pressure regulation in humans. Trends Endocrinol Metab. 2008; 19:91–95. [PubMed: 18280177]

28. McCormick JA, Yang CL, Ellison DH. WNK kinases and renal sodium transport in health and disease: an integrated view. Hypertension. 2008; 51:588–596. [PubMed: 18212265]

29. Vitari AC, Deak M, Morrice NA, Alessi DR. The WNK1 and WNK4 protein kinases that are mutated in Gordon's hypertension syndrome phosphorylate and activate SPAK and OSR1 protein kinases. Biochem J. 2005; 391:17–24. [PubMed: 16083423]

30. San-Cristobal P, Pacheco-Alvarez D, Richardson C, Ring AM, Vazquez N, Rafiqi FH, Chari D, Kahle KT, Leng Q, Bobadilla NA, Hebert SC, Alessi DR, Lifton RP, Gamba G. Angiotensin II signaling increases activity of the renal Na-Cl cotransporter through a WNK4-SPAK-dependent pathway. Proc Natl Acad Sci U S A. 2009; 106:4384–4389. [PubMed: 19240212]

31. Shaharabany M, Holtzman EJ, Mayan H, Hirschberg K, Seger R, Farfel Z. Distinct pathways for the involvement of WNK4 in the signaling of hypertonicity and EGF. Febs J. 2008; 275:1631–1642. [PubMed: 18312414]

32. Hoorn EJ, Nelson JH, McCormick JA, Ellison DH. The WNK kinase network regulating sodium, potassium, and blood pressure. J Am Soc Nephrol. 2011; 22:605–614. [PubMed: 21436285]

33. Vitari AC, Deak M, Collins BJ, Morrice N, Prescott AR, Phelan A, Humphreys S, Alessi DR. WNK1, the kinase mutated in an inherited high-blood-pressure syndrome, is a novel PKB (protein kinase B)/Akt substrate. Biochem J. 2004; 378:257–268. [PubMed: 14611643]

34. Phillips MS, Liu Q, Hammond HA, Dugan V, Hey PJ, Caskey CJ, Hess JF. Leptin receptor missense mutation in the fatty Zucker rat. Nat Genet. 1996; 13:18–19. [PubMed: 8673096]

35. Komers R, Zdychova J, Cahova M, Kazdova L, Lindsley JN, Anderson S. Renal cyclooxygenase-2 in obese Zucker (fatty) rats. Kidney Int. 2005; 67:2151–2158. [PubMed: 15882258]

36. Anderson S, Chapman JG, Oyama TT, Komers R. Effect of orchiectomy on renal function in control and diabetic rats with chronic inhibition of nitric oxide. Clin Exp Pharmacol Physiol. 2010; 37:19–23. [PubMed: 19473197]

37. Rinehart J, Maksimova YD, Tanis JE, Stone KL, Hodson CA, Zhang J, Risinger M, Pan W, Wu D, Colangelo CM, Forbush B, Joiner CH, Gulcicek EE, Gallagher PG, Lifton RP. Sites of regulated phosphorylation that control K-Cl cotransporter activity. Cell. 2009; 138:525–536. [PubMed: 19665974]

38. Ko B, Joshi LM, Cooke LL, Vazquez N, Musch MW, Hebert SC, Gamba G, Hoover RS. Phorbol ester stimulation of RasGRP1 regulates the sodium-chloride cotransporter by a PKC-independent pathway. Proc Natl Acad Sci U S A. 2007; 104:20120–20125. [PubMed: 18077438]

39. Hadchouel J, Soukaseum C, Busst C, Zhou XO, Baudrie V, Zurrer T, Cambillau M, Elghozi JL, Lifton RP, Loffing J, Jeunemaitre X. Decreased ENaC expression compensates the increased NCC activity following inactivation of the kidney-specific isoform of WNK1 and prevents hypertension. Proc Natl Acad Sci U S A. 107:18109–18114. [PubMed: 20921400]

40. Komers R, Schutzer WE, Reed JF, Lindsley JN, Oyama TT, Buck DC, Mader SL, Anderson S. Altered endothelial nitric oxide synthase targeting and conformation and caveolin-1 expression in the diabetic kidney. Diabetes. 2006; 55:1651–1659. [PubMed: 16731827]

41. Yang CL, Zhu X, Ellison DH. The thiazide-sensitive Na-Cl cotransporter is regulated by a WNK kinase signaling complex. J Clin Invest. 2007; 117:3403–3411. [PubMed: 17975670]

42. Piechotta K, Lu J, Delpire E. Cation chloride cotransporters interact with the stress-related kinases Ste20-related proline-alanine-rich kinase (SPAK) and oxidative stress response 1 (OSR1). J Biol Chem. 2002; 277:50812–50819. [PubMed: 12386165]

43. McCormick JA, Mutig K, Nelson JH, Saritas T, Hoorn EJ, Yang CL, Rogers S, Curry J, Delpire E, Bachmann S, Ellison DH. A SPAK isoform switch modulates renal salt transport and blood pressure. Cell Metab. 2011; 14:352–364. [PubMed: 21907141]

44. Zdychova J, Komers R. Emerging role of Akt kinase/protein kinase B signaling in pathophysiology of diabetes and its complications. Physiol Res. 2005; 54:1–16. [PubMed: 15717836]

45. Kunchaparty S, Palcso M, Berkman J, Velazquez H, Desir GV, Bernstein P, Reilly RF, Ellison DH. Defective processing and expression of thiazide-sensitive Na-Cl cotransporter as a cause of Gitelman's syndrome. Am J Physiol. 1999; 277:F643–649. [PubMed: 10516289]

46. Sandberg MB, Maunsbach AB, McDonough AA. Redistribution of distal tubule Na+-Cl- cotransporter (NCC) in response to a high-salt diet. Am J Physiol Renal Physiol. 2006; 291:F503–508. [PubMed: 16554416]

47. Mutig K, Saritas T, Uchida S, Kahl T, Borowski T, Paliege A, Bohlick A, Bleich M, Shan Q, Bachmann S. Short-term stimulation of the thiazide-sensitive Na+-Cl- cotransporter by vasopressin involves phosphorylation and membrane translocation. Am J Physiol Renal Physiol. 2010; 298:F502–509. [PubMed: 20007345]

48. Pickkers P, Garcha RS, Schachter M, Smits P, Hughes AD. Inhibition of carbonic anhydrase accounts for the direct vascular effects of hydrochlorothiazide. Hypertension. 1999; 33:1043–1048. [PubMed: 10205245]

49. Madala Halagappa VK, Tiwari S, Riazi S, Hu X, Ecelbarger CM. Chronic candesartan alters expression and activity of NKCC2, NCC, and ENaC in the obese Zucker rat. Am J Physiol Renal Physiol. 2008; 294:F1222–1231. [PubMed: 18305093]

50. Bickel CA, Verbalis JG, Knepper MA, Ecelbarger CA. Increased renal Na-K-ATPase, NCC, and beta-ENaC abundance in obese Zucker rats. Am J Physiol Renal Physiol. 2001; 281:F639–648. [PubMed: 11553510]

51. van der Lubbe N, Lim CH, Fenton RA, Meima ME, Jan Danser AH, Zietse R, Hoorn EJ. Angiotensin II induces phosphorylation of the thiazide-sensitive sodium chloride cotransporter independent of aldosterone. Kidney Int. 2011; 79:66–76. [PubMed: 20720527]

52. Subramanya AR, Liu J, Ellison DH, Wade JB, Welling PA. WNK4 diverts the thiazide-sensitive NaCl cotransporter to the lysosome and stimulates AP-3 interaction. J Biol Chem. 2009; 284:18471–18480. [PubMed: 19401467]

53. Sohara E, Rai T, Yang SS, Ohta A, Naito S, Chiga M, Nomura N, Lin SH, Vandewalle A, Ohta E, Sasaki S, Uchida S. Acute insulin stimulation induces phosphorylation of the Na-Cl cotransporter in cultured distal mpkDCT cells and mouse kidney. PLoS One. 2011; 6:e24277. [PubMed: 21909387]

54. Ohta A, Rai T, Yui N, Chiga M, Yang SS, Lin SH, Sohara E, Sasaki S, Uchida S. Targeted disruption of the Wnk4 gene decreases phosphorylation of Na-Cl cotransporter, increases Na excretion and lowers blood pressure. Hum Mol Genet. 2009; 18:3978–3986. [PubMed: 19633012]

55. Yang CL, Zhu X, Wang Z, Subramanya AR, Ellison DH. Mechanisms of WNK1 and WNK4 interaction in the regulation of thiazide-sensitive NaCl cotransport. J Clin Invest. 2005; 115:1379–1387. [PubMed: 15841204]
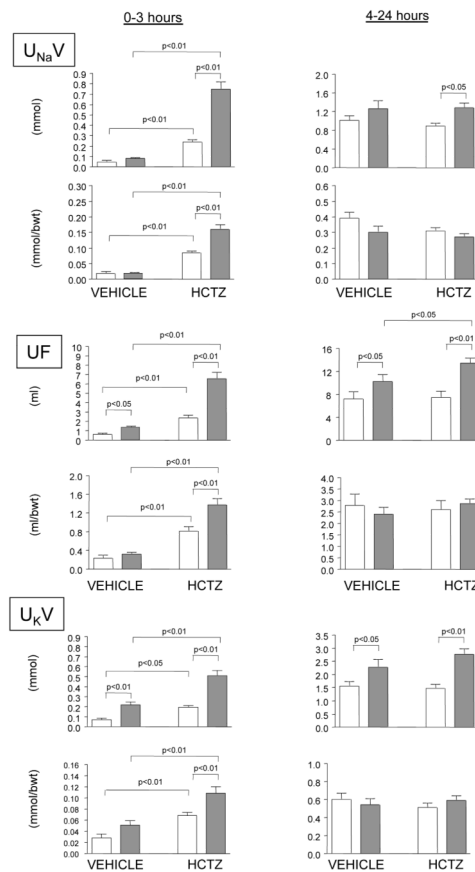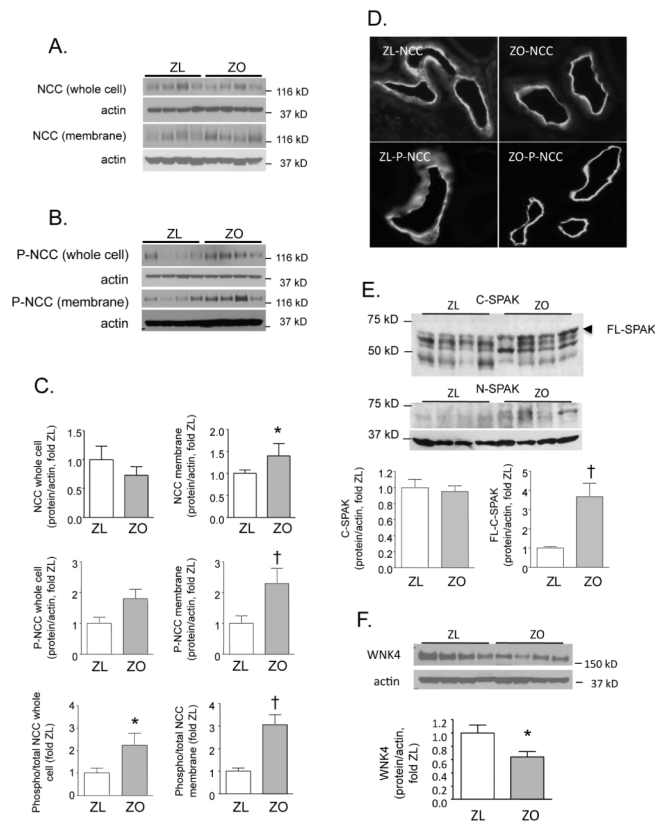
Figure 1.
Natriuretic responses to vehicle and hydrochlorothiazide (HCTZ) in Zucker lean and obese rats. Zucker lean (blank columns) and obese (filled columns) rats were administered with a vehicle (200 µl of normal saline) and placed into metabolic cages for 24 hours. The urine was collected during the early 3-hour period (left panels) and for the rest of the 24-hour collection period for determination of urinary sodium excretion ($U_{Na}V$), urinary flow (UF) and urinary potassium excretion (U_KV). The following week the measurements were repeated after the administration HCTZ (3.75 mg/kg). The data are expressed in absolute values and as ratio per body weight.
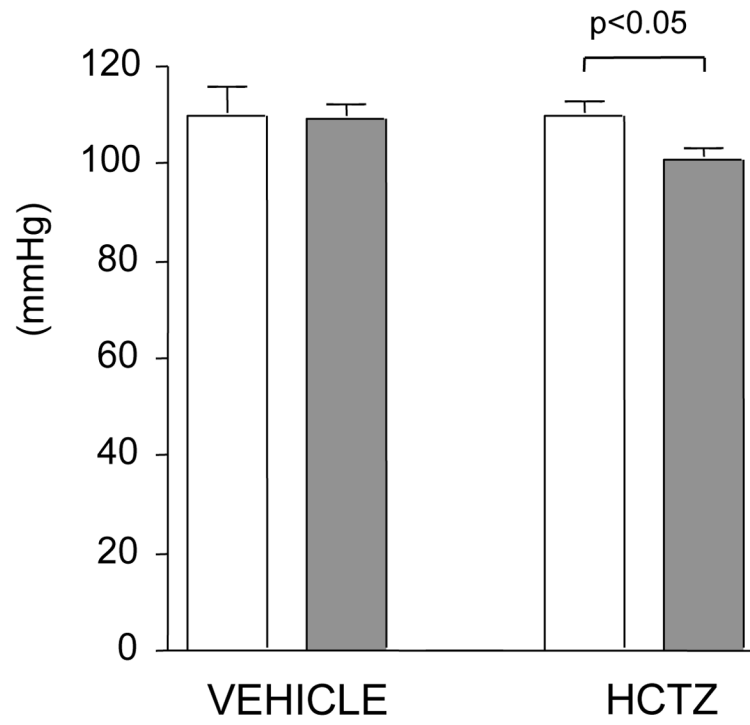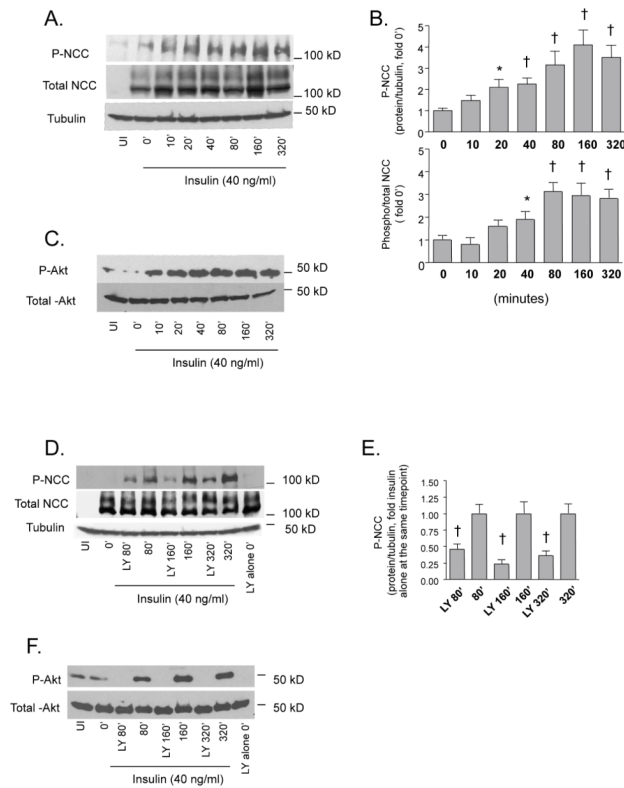
Figure 2.
Systolic blood pressure in Zucker lean (empty bars) and obese (filled bars) rats administered with a vehicle (0.9% NaCl, 200 μl i.p.) or hydrochlorothiazide (HCTZ, 3.75 mg/kg i.p. in 200 μl 0.9% NaCl).

Figure 3. Renal cortical protein expression of NCC, SPAK and WNK4 in Zucker lean (ZL) and obese (ZO) rats

A. Total NCC protein abundance and **B.** Thr53 phosphorylation of the NCC (P-NCC) were analyzed by western blotting in whole cell and crude membrane fractions. **C.** Graphed results of densitometric analysis of NCC and P-NCC abundance expressed as a ratio of protein/actin (loading control) or as a ratio of phospho- and total NCC (*p<0.05, †p<0.01 vs. ZL). **D.** The NCC and P-NCC were localized in the DCT by immunofluorescence microscopy. **E.** Western blot analysis of renal cortical homogenates using primary antibodies against C- and N-termini of SPAK. The graph shows densitometric analysis of all C-SPAK bands and the band with the highest molecular weight (~ 60 kD), corresponding to full size SPAK (FL-SPAK) (†p<0.01 vs. ZL). **F.** Renal protein expression of WNK4 in ZL and ZO rats. The graph shows the results of densitometric analysis of western blots. Representative blots are shown in insets (*p<0.05 vs. ZL).

Figure 4. Effect of insulin on NCC and Akt kinase phosphorylation in *FlpIn NCC* cells
A. Immunoblot analysis phospho-Thr53/55 (P-NCC) and total NCC. To study the effect of insulin on NCC phosphorylation *in vitro*, the *FlpIn NCC* cells were first stimulated with tetracycline to induce NCC expression. Eighteen hours after NCC induction the cells harvested at baseline (0 minutes) or stimulated with insulin (40 ng/ml), harvested after 10–360 minutes, and analyzed by immunoblotting using primary antibodies raised against P-NCC and total NCC. Uninduced cells (UI) were harvested for western blots as negative controls. Tubulin was used as a loading control. **B.** Densitometric analysis of P-NCC abundance (P-NCC/tubulin ratio) and a ratio of phospho- and total NCC (*p<0.05, †p<0.01 vs. baseline (0′)). **C.** The Ser473 Akt phosphorylation (P-Akt) in response to insulin stimulation was also determined in *FlpIn NCC* cells as an established step in insulin signaling cascade. Total Akt protein abundance was analyzed as loading control. **D**. The effects of insulin on NCC phosphorylation were further investigated in tetracycline-induced cells with or without pretreatment with the phosphatidyl-inositol-3 kinase (PI3K) inhibitor LY294002 (LY, 60 min., 50 μM). The figure shows representative blot after 80–320 min. of insulin stimulation. **E**. Densitometric analysis of P-NCC abundance (P-NCC/tubulin ratio) in insulin stimulated cells with or without LY pretreatment. Since the baseline NCC phosphorylation was hardly detectable in this experiment, the P-NCC abundance in LY-pretreated cells is for each time point presented as a proportion of P-NCC abundance in insulin-stimulated cells without LY pretreatment (†p<0.01 vs. insulin treated cells at the same time point). **F**. Immunoblot of P-Akt and total Akt in insulin-stimulated cells with and without LY pretreatment.
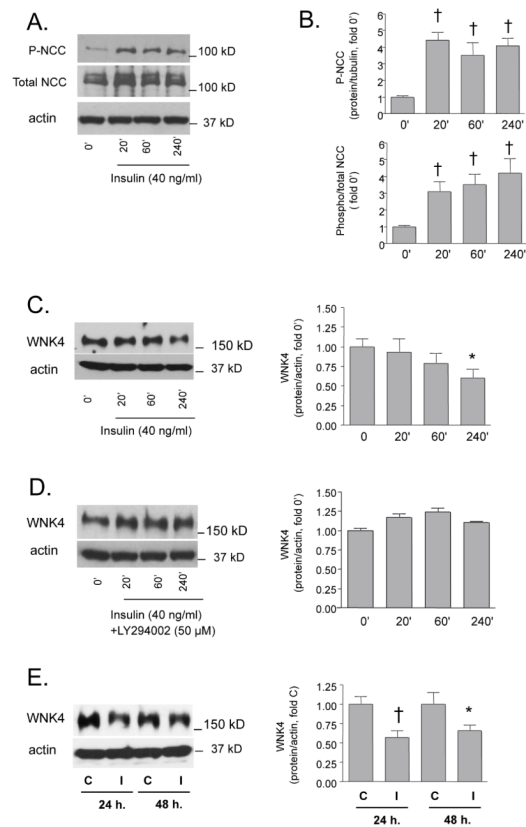
Figure 5. Effect of insulin on Thr 53/55 NCC phosphorylation and WNK4 expression in *MDCT* cells

The MDCT cells were used as another *in vitro* mammalian cell model, which displays endogenous NCC and WNK4 expression. The cells were stimulated with insulin (40 ng/ml) for 20, 40 and 240 minutes. At the selected time points, the cells were harvested and analyzed by immunoblotting. **A.** Immunoblot analysis of phospho-Thr53/55 (P-NCC) and total NCC. **B.** Densitometric analysis of P-NCC abundance and a ratio of phospho- and total NCC ([†]p<0.01 vs. baseline (0′)). **C.** Immunoblot analysis of WNK4 protein abundance in insulin-stimulated cells. The figure shows representative blot (left) and densitometric analysis (right, *p<0.05 vs. baseline (0′)). **D.** Representative immunoblot and densitometry of WNK4 protein abundance in insulin-induced cells pretreated with the PI3K inhibitor LY294002 (LY, 60 min., 50 μM). **E.** Representative immunoblot and densitometric analysis of WNK4 protein abundance in cells grown in insulin-free (C) and insulin-containing media (I) for 24 and 48 hours (*p<0.05, [†]p<0.01 vs. C).

Table 1

General physical and metabolic characteristics

	Body Weight (g)	Kidney Weight (mg)	Plasma Insulin (ng/ml)	Blood Glucose (mmol/l)	Plasma Aldosterone (nM)
ZL	358±9	1127±46	3.0±0.6	5.3±0.1	2.28 ±0.30
ZO	538±24 *	1295±44 *	40.8±14.0 *	6.7±0.3 *	2.24±0.27

*
p<0.05